Relaxation of cold plasmas and threshold lowering effect

Yukap Hahn
TRG, 5916 Old Greenway Drive, Glen Allen, Virginia 23059
(Received 14 March 2001; revised manuscript received 29 June 2001; published 26 September 2001)

Low temperature plasmas are produced by photoionization of cold trapped atoms. Due to the threshold energy shift caused by overlapping ion fields, the effective kinetic energy of the free electrons is increased by $\Delta_P = 2C_P/a$, where a is the Wigner-Seitz radius and $C_P \simeq 11$ is a universal constant. Detailed discussion is given on the self-consistent determination of C_P, using a Debye shielded, fluctuating lattice model. The attainable minimum electron temperature is given by the plasma density alone, as $T_e \simeq \Delta_P/3 \simeq 7/a$. No Wigner crystallization is possible in such plasmas, unless a strong confining external field is present. The shift imposes a stringent cutoff on the high Rydberg state contributions to the three-body recombination probabilities, and a new estimate of the rates is presented. For a freely expanding cold plasma, an additional mode of adiabatic motional recombination is found to dominate plasma relaxation.

DOI: 10.1103/PhysRevE.64.046409 PACS number(s): 52.20.−j, 34.10.+x, 34.80.Kw

I. INTRODUCTION

Recent advances [1–3] in cooling trapped atoms have opened up many new areas of research, that include the Bose-Einstein condensation and laser manipulated excitations. In particular, ionization of cold atoms by laser irradiation presumably produces plasmas of precisely controlled temperature [4–6]. Typical atomic density realized experimentally is $10^6 - 10^{11}\,\mathrm{cm}^{-3}$, and up to 25% of these atoms are usually ionized. Electron temperature T_0 of the plasma thus created can be in the Kelvin range. Alternative to direct photoionization, cold plasmas (CP) may also be produced by first laser excition of cold trapped atoms to high Rydberg states, which can subsequently turn into a plasma [7] via Penning ionization. This may be further followed by collisional ionization and recombination. Plasmas of such low T_0 pose many new and interesting physical problems, especially when they are not quite in thermal equilibrium and expanding in absence of confining fields.

Cold plasmas can relax by various modes of recombination [8], the radiative recombination, three-body recombination, and possibly by dielectronic recombination. We study in this report the relaxation of CP by analyzing some of the properties unique to such plasmas [9]. At extremely low temperature, the threshold lowering effect plays a crucial role [9,10], as it manifests itself in magnified form and imposes various constraints on the relaxation processes. The kinetic energies of the free electrons and ions are shifted, and various recombination processes are suppressed. However, the earlier work of Ref. [10] turned out to be insufficient to describe a transient condition of interest here. Incidentally, possible importance of this effect was noted previously [8] in connection with the recombination at low T.

In absence of confining potentials, the plasma expands under its own pressure, and the free electrons with energies less than the shift Δ_P are trapped. As the plasma expands, the shift decreases, the potential barrier of the ions is raised, and trapped electrons are converted to ''bound'' electrons. The trapping of electrons by an expanding plasma potential generates a new mode of recombination, the adiabatic motional recombination. On the other hand, for a plasma spatially confined by a trapping field, such a mode is absent and the three-body recombination is expected to be dominant.

We discuss in detail the threshold lowering effect (TLE) in Sec. II, where a self-consistent procedure for the determination of the energy shift is developed. A theoretical explanation of the various anomalies observed in a recent experiment [6] is given in terms of the TLE. Although the model introduced in Sec. II is crude, the physical picture that evolves is quite general and the parameter C_P of the shift seems to be a universal constant and intrinsic property of the CP. The various recombination probabilities are estimated in Sec. III, taking the TLE into account. Generally, the TLE reduces the rates. The adiabatic motional recombination process is described in Sec. IV and its probability is estimated and compared with that of other recombination processes.

II. THRESHOLD LOWERING EFFECT

We first discuss the TLE [9], which affects the dynamics of CP by suppressing the various recombination processes. The previous study of TLE is given, for example, by Stewart and Pyatt [10], in which the nonlinear Poisson-Maxwell equation was solved to obtain the screened electric potential of the central ions, and the threshold lowering values are extracted. However, the transient plasma of interest here is not quite in thermal equilibrium, especially when the plasma starts to expand under its own pressure as soon as it is created, in the time scale of $10^{-6} - 10^{-7}$ sec. Therefore, the energy shift estimated under the equilibrium condition is not adequate to describe the observed data. A new model is required to describe the present situation, in which T is not well defined and the usual Poisson equation is not quite applicable.

When the temperature of the trapped atoms to be ionized is very low, typically in the mK range, the thermal motion of the atoms may be neglected in first approximation. Since the TLE is mainly caused by the overlapping ion fields, it is convenient to assume that the ions produced by photoionization of near stationary atoms are initially situated on lattice sites with the spacing of roughly $2a$, where a is the Wigner-Seitz radius defined by $a = (3/4\pi N)^{1/3}$ and N is the ion den-

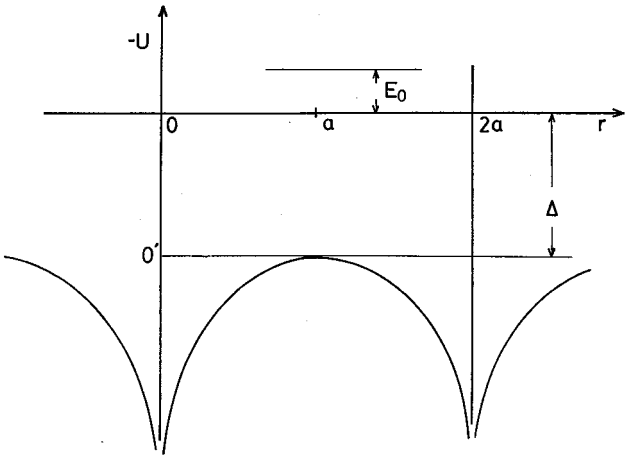

FIG. 1. The TLE is illustrated for the case of two overlapping ionic potentials. The new threshold O' is shifted down by the amount Δ from the original point O for the unperturbed central ion located at $r=0$. The second ion is located at $r=2a$. E_0 is the excess energy gained by the ionized electron from the laser photons. The apparent energy available is then $E_0+\Delta$.

sity $N_I \simeq N \simeq N_e$ for the assumed neutrality. We start the construction of a model with a pair of ions and gradually add on the many-ion effect as well as the Debye screening and random thermal motion of the plasma ions.

For a pair of ions, the potential near the midpoint $r=a$ is given by $U_2(r)=1/r+1/(2a-r)$. This gives a down shift (Fig. 1) in the ionization threshold for the electrons, from O to O', by $\Delta_2 \equiv U_2(r=a)=2/a$. Next, in extending this model to the case of many ions, we assume that the overall lattice geometry for the ions is not changed, so that the symmetry around the point $r=a$ for the two-ion case is maintained. Then the potential at $r=a$ is modified to a form $U_\infty(r) \simeq U_2(r) b(\eta)$, where η is the Debye radius given in units of a, as $\eta = r_D/a$ with $r_D = \sqrt{T_e/4\pi N_e}$; the usual plasma parameter $\Gamma = 1/aT_e$ is related to η as $\eta^2 = 1/3\Gamma$. Presumably, the effect of many ions on U is to flatten the shape of the bump at $r \simeq a$ and makes the shift larger.

In addition, thermal motion of the plasma ions with their mutual interaction produces fluctuations about the lattice sites. After all, the lattice model may be an over simplification, valid in the zero-temperature limit. The ion motion affects on average the interionic separation $2a$. We incorporate the effect by attaching a factor $1/d(\eta)$ in U. The ion-ion distribution function $g_{II}(\eta)$ obtained by the density functional calculation [11–13] contains the necessary information to parametrize d (see Fig. 2), although a gross extrapolation in the plasma parameter space is made.

Thus, finally we have

$$U(r)=2C(\eta)/a, \quad \text{with} \quad C(\eta)=b(\eta)/d(\eta). \tag{1}$$

A simple model was constructed [9] for evaluation of b that reflects the ion distribution and Debye screening. That is, the function $b(\eta)$ is written in two parts

$$b(\eta)=b_0+b_s(\eta), \tag{2a}$$

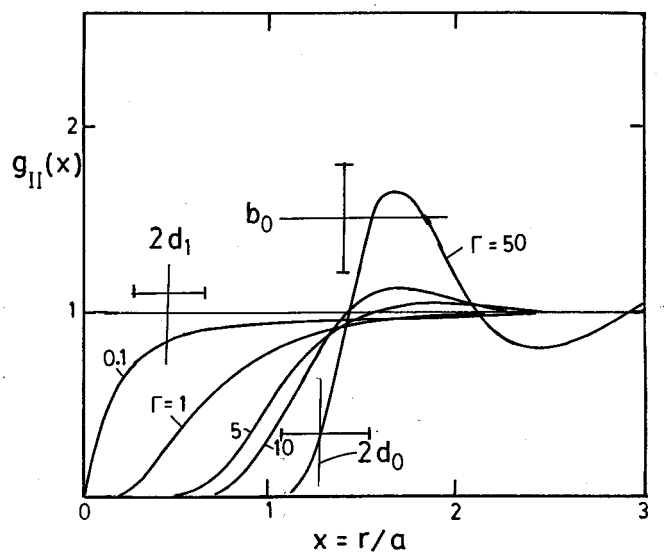

FIG. 2. Parametrization of d_0, d_1, and b_0 is carried out using the results of Refs. [11–13]. Plotted is the ion pair distribution function $g_{II}(r,\Gamma)$ that describes the probability of finding an ion from the central ion that is located at $x=0$, where $x=r/a$. $\Gamma = Z^2/aT$. The horizontal line marks the value of b_0, with probable uncertainty indicated. The two vertical lines specify the parameters d_0 and d_1. Note that $\Gamma/Z^2 = g = 1/3\eta^2$. In the present case, $Z=1$.

where the large η contribution is contained in b_s, and b_0 is to be parametrized later to account for the physics at $\eta<1$. We construct a simple model for b_s as

$$b_s(\eta)=\sum_{n=1}^{\infty}\sum_{l=0}^{m}\sum_{m=0}^{\infty} f_{lmn}\exp(-s_{lmn}/\eta_{lmn})/s_{lmn}, \tag{2b}$$

where $s_{lmn}=\sqrt{(2n-1)^2+l^2+m^2}$. The weight factors are $f_{00n}=1$, $f_{0mn}=f_{m0n}=2$, $f_{mmm}=4$, and $f_{lmn}=4$, for $n>0$ and $l,m \geqslant 0$. Furthermore, $\eta_{lmn}=\eta/(1+\eta_1 s_{lmn})$, where η_1 is a parameter that is to take into account the shadow effect of dressed ions that lie in the pathway between the central and distant ions. (Of course, this effect is not present if the ions are bare.) Values for η_1 between 0.01 and 0.05 have been tried; the final result is not too sensitive to this parameter, and in the following we simply set $\eta_1 \simeq 0.03$. Thus, form (2b) for b_s explicitly contains both the many-ion and screening factors. Now, we parametrize b_0. The behavior of b_s at small η is found to be $b_s \to 0$ as $\eta \to 0$, indicating that Eq. (2b) is not reliable at small η; this is expected because a simple Debye screening adopted here is probably not correct for small η in the strong coupling limit, where all the particles are very much ''localized.'' To rectify this deficiency, we have added b_0, whose value is determined from the result of Refs. [11–13], as illustrated in Fig. 2. Approximately, $b_0 \simeq 1.5$ is chosen.

Function $d(\eta)$ in U of Eq. (1) is to reflect on the fact that the ions move around and can be found nearer to the central ion. Again, the density functional theory provides the necessary information, especially in the high Γ (i.e., in the small η) limit. We fitted the result in a form convenient for our

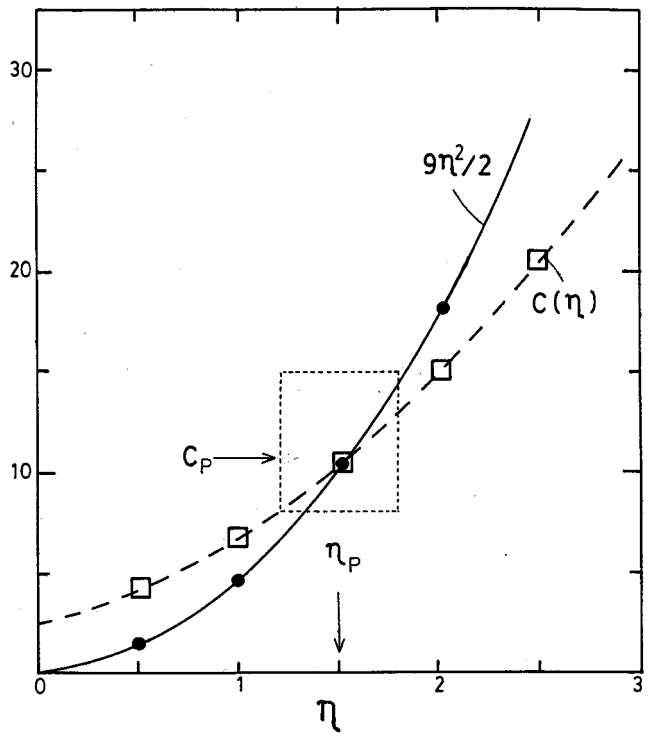

FIG. 3. Determination of Δ_P and η_P. The model described by Eqs. (1) and (2) are solved iteratively for η and Δ, until a self-consistency is achieved. The converged values are denoted by η_P and C_P. Estimated uncertainty is indicated by a dotted square.

purpose $d(\eta) \simeq (d_0 + d_1\eta)/(1+\eta)$, with $2d_0 \simeq 1.2$ and $2d_1 \simeq 0.5$, as shown also in Fig. 2.

In the determination of parameters d_0, d_1, and b_0, it is important to keep in mind that the results of the density functional theory calculations of Refs. [11–13] are for high $N \simeq 10^{25}\,\mathrm{cm}^{-3}$ and high $T \geqslant 1$ eV. The CP of interest here is in the opposite end of the parameter spectrum. In the absence of data of direct relevance to the present case, a gross extrapolation has to be made to very low N and low T region. Although a similar scaling of the theory in Γ is assumed, adoption of the existing results requires extra caution. New detailed calculations for CP are warranted.

Expression for $C(\eta)$ in Δ is given in terms of the functions b and d, both of which depend sensitively on the variable $\eta = 1/\sqrt{3\Gamma}$. On the other hand, η itself depends on the electron temperature T_e through r_D, which is in turn derived from Δ, as $T_e \simeq \Delta/3$. Therefore, we have the situation in which a self-consistent determination of Δ and η is required. That is, for given η from an assumed T_e, and b_s and C are calculated, which give Δ. This Δ in turn is used to evaluate a new T_e and then a new η. This procedure must be repeated until a full self-consistency is achieved between η, Δ, and T_e. We denote the final converged values by subscript P. This is illustrated in Fig. 3, where $C_P \simeq 11 \pm 5$ and $\eta_P \simeq 1.5 \pm 0.4$. The corresponding values for b and d are $b_P \simeq 4.1$ and $d_P \simeq 0.39$. In view of the approximations introduced in the parametrization, the crudity of the model, and a giant extrapolation of the high density result to the present case, there are considerable uncertainties in these values. However, most of the crucial physics for this complex system have been incorporated. By contrast, the Δ' given by Stewart and Pyatt [10] for a plasma in equilibrium gives a value roughly ten times smaller than Δ_P.

The total energy available to the system immediately after the CP production is given by the sum of the excess energy $E_0 = E_{\mathrm{laser}} - E_{\mathrm{ioniz}}$ of the photoionization and the energy shift Δ_P, as

$$E = E_0 + \Delta_P, \tag{3}$$

provided the plasma edge effect is negligible. The shift in the ionization threshold is valid under the assumption that the plasma volume is large and the edge effect is small. During the thermalization, which takes place roughly in 10^{-7}–10^{-6} sec, depending on the plasma parameters [8], the total available energy E of Eq. (3) is assumed to be shared among the electrons and ions, and possible by the neutrals that are present in abundance. We thus simply set

$$E_I \simeq E_e \simeq E/2 \quad \text{and} \quad T_e \simeq T_I \simeq E/3. \tag{4}$$

In case the neutrals participate in the energy sharing, the resulting energies and temperatures would be less than that given by Eq. (4).

The TLE and its consequence have been shown [9] to explain most of the anomalies observed in a recent experiment [6]. In particular, the expansion velocity v_I of the ions at low temperature is given by Δ_P, as $v_I \simeq \sqrt{\Delta_P/M}$, while for large E_0, $v_I \simeq \sqrt{E_0/M}$. They are consistent with experimental data. The density dependence at low E_0 is $v_I \propto 1/\sqrt{a} \propto N_I^{1/6}$, which also agrees with observation. As will be discussed in Sec. IV, the model can be used to describe a dominant relaxation mechanism in the case of an expanding plasma.

We comment on several additional features predicted by the TLE model: (i) At low E_0, the minimum attainable plasma temperature is completely determined by the plasma density. That is, $T_e \simeq (2C_P/3)/a \simeq 7/a \equiv T_{e,\min}$. In the absence of any plasma confining fields, the lowest plasma temperature cannot be made arbitrarily low. For example, at $a = 10^5 a_B$ corresponding to roughly $N \simeq 10^9\,\mathrm{cm}^{-3}$, we have $\min T_e \simeq 20\,\mathrm{K}$. (ii) It is noted that the parameter $C_P \simeq 11$ seems to assume a universal character, just as the Madelung constant in solids. It does not depend on η, because C_P and η_P are determined by the self-consistent procedure. (iii) Cold plasmas with the above behavior have the plasma parameter $\Gamma < \max \Gamma = 0.15$, so that Wigner crystallization of such plasmas (at $\Gamma \simeq 150$ corresponding to $\eta \simeq 0.05$) is not possible. We recall that $\eta^2 = 1/3\Gamma$, with $\Gamma = 1/(ak_BT_e)$.

III. RADIATIVE AND THREE-BODY RECOMBINATIONS

The main consequences of the TLE on the various recombination processes are expected to be twofold: (a) The kinetic energy of the electrons is shifted to the new value $E_e \simeq (E_0 + \Delta_P)/2$ and the temperature $T_e \simeq 2E_e/3$, from Eqs. (3) and (4). Generally, a larger kinetic energy reduces the rates. As stressed earlier, in the limit of small E_0, the electron temperature is mainly determined by the electron density

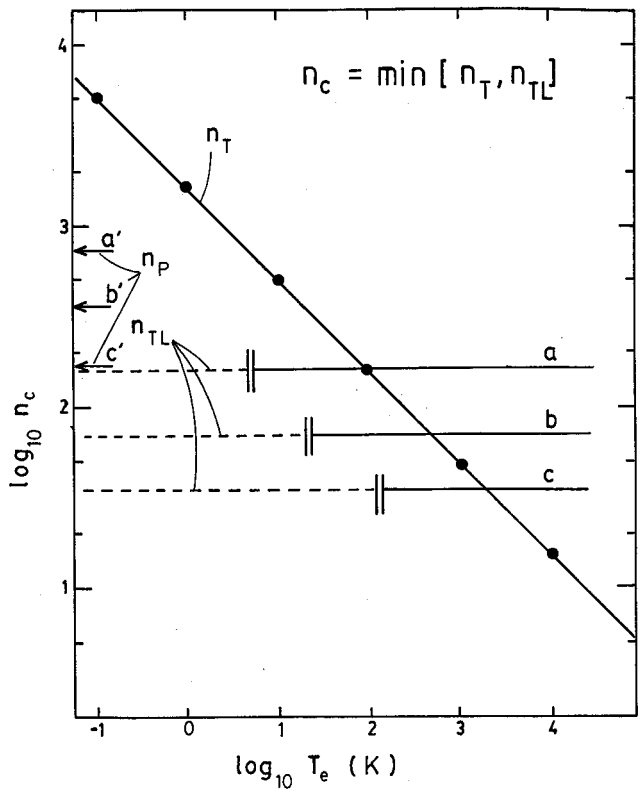

FIG. 4. The TLE imposes a new HRS cutoff n_{TL}. Curves *a*, *b*, and *c* are for three densities, $N \simeq 10^7$, 10^9, and $10^{11}\,\mathrm{cm}^{-3}$, respectively. The lines with a', b', and c' indicates the cutoff used earlier in Ref. [9] without the TLE, i.e., n_P that is larger than n_{TL} by a factor of 4.7. The vertical double bars indicate the $T_{e,\min}$ as dictated by TLE.

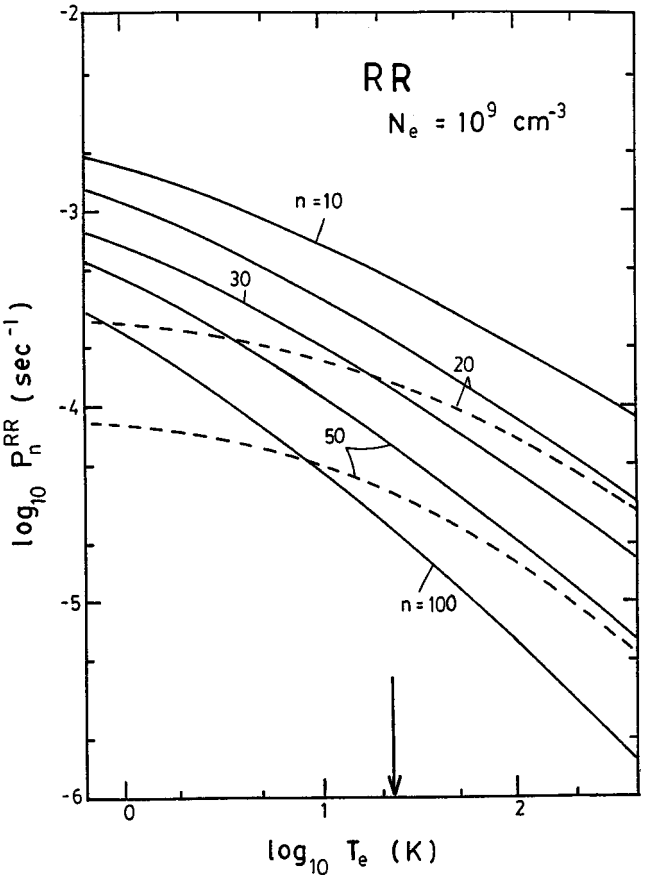

FIG. 5. The RR probabilities without the TLE are given (solid lines) as functions of temperature, for different principal quantum number *n* of the recombined states, for $n=10$, 20, 30, 50, and 100. Reductions of P_n^{RR} are illustrated for $n=20$ and 50 (dashed lines), all for the electron density of $N_e \simeq 10^9\,\mathrm{cm}^{-3}$. The corresponding electron temperature of 22 K is indicated by the arrow, for the case of $E_0=0$.

through the factor $1/a$ in Δ_P. (b) Since the TLE moves the ionization threshold down to O' (see Fig. 1) at $-\Delta_P$, all the high Rydberg states (HRS) of the original ions that lie between O and O' are erased and become continuum states, so that they are no longer available for recombination. This is incorporated in terms of a new HRS cutoff $n_{TL} \simeq 1/\sqrt{\Delta_P}$. Figure 4 illustrates this change. Explicitly, at low E_0, $n_{TL} \simeq n_P/4.65$, where $n_P = \sqrt{a}$ is the cutoff that corresponds to the ion packing [8]. Obviously, $n_{TL} < n_P$, and this affects HRS most.

The radiative recombination (RR) probability P^{RR} is defined in terms of its rate α^{RR} by

$$P^{RR}(\mathrm{sec}^{-1}) \simeq N_e \alpha^{RR}(\mathrm{cm}^3/\mathrm{sec}), \tag{5}$$

which shows explicitly the density dependence; α^{RR} is independent of *N*. The simple Kramer's formula for the RR cross section provides a convenient reference point of discussion for low *T* plasmas; $\sigma_n^{RR,K} \simeq 32/(3\sqrt{3})\alpha_0^3\beta^4/[n(\beta^2+n^2)]\pi a_B^3$, where *n* denotes the principal quantum number of states of the recombined ion and β is inverse of wave number of the continuum electron before capture, $\beta = 1/ka_B = 1/\sqrt{2E}$ in a.u. Reliability of this formula, as well as an extension for the dependence on angular momentum *l*, has been examined in detail in Ref. [8]. The RR process is generally slow as compared to the radiationless recombination mode, the three-body recombination (TBR), for plasmas of moderate densities, and favors recombination to low-lying states of the ions. That is, for large *n* but $\beta < n$, $\sigma^{RR} \propto n^{-3}$. But for $\beta > n$, the *n* dependence is much slower, $\sigma^{RR} \propto 1/n$. In Fig. 5, we compare the RR probability P_n^{RR} with and without the TLE. The *P*'s without the TLE are plotted as functions of T_e for $n=10$ to 100, by solid lines. The TLE on RR are shown explicitly for the case $n=20$ and 50 by dashed lines, where for illustration $N_e \simeq 10^9\,\mathrm{cm}^{-3}$ is assumed. Of course, due to $n_{TL} \simeq 74$, the entry for $n=100$ is no longer applicable when TLE is operative. The TLE is mainly to increase the kinetic energy of the continuum electrons, from $E_e \simeq E_0/2$ to $(E_0+\Delta_P)/2$. The high *n* cutoff has only a minor effect on RR. Nevertheless, the RR starts to be relatively more important at lower densities, for example, for $N_e \simeq N_I \simeq 10^4\,\mathrm{cm}^{-3}$ and for highly charged ions. It may even dominate over TBR.

The TBR is known to dominate recombination of electrons to HRS of the target ions, while the RR predominantly fills the low-lying states of the target ions. It is responsible for rapidly attaining Saha equilibrium for HRS near the

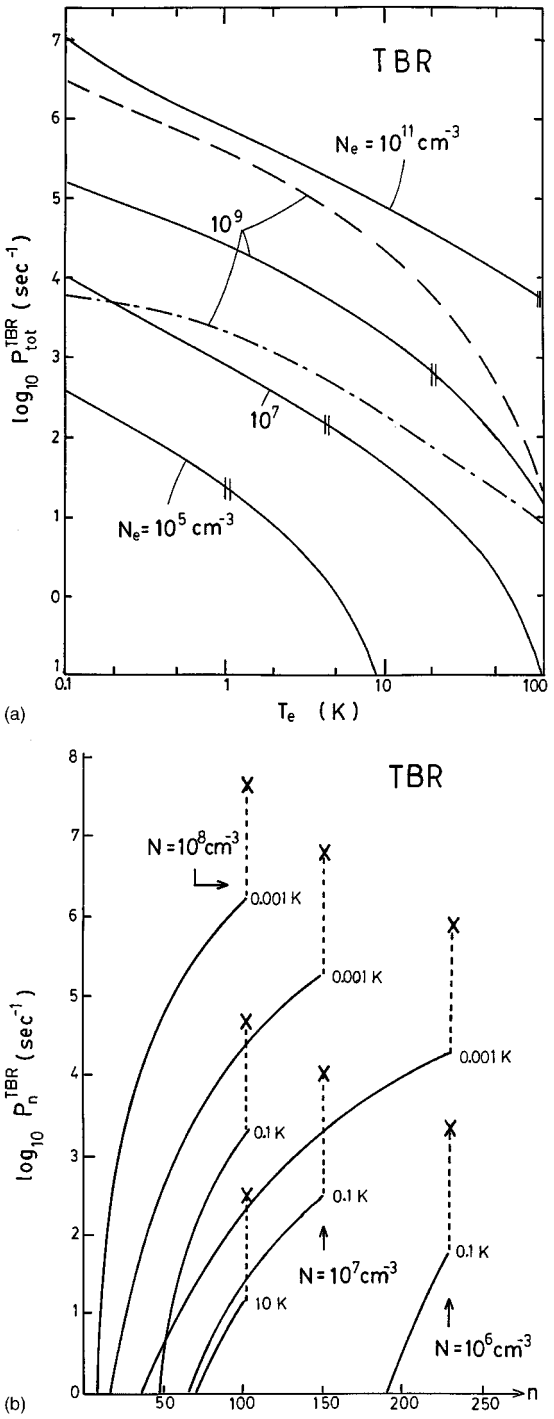

FIG. 6. (a) The total TBR probabilities are given as functions of T_e for four different densities, $N_e = 10^5$. 10^7, 10^9, and $10^{11}\,\mathrm{cm}^{-3}$. The solid lines are obtained with the HRS cutoff n_{TL}. The effect of alternate cutoffs, n'_{TL} and n''_{TL} are illustrated by dashed lines, for the case $N_e \simeq 10^9\,\mathrm{cm}^{-3}$. (b) The TBR probabilities are given as functions of the principal quantum number n of the recombined atoms, for three different densities, $N_e = 10^6$, 10^7, and $10^8\,\mathrm{cm}^{-3}$. The temperatures are very low, showing the dependence on T as well as on n and N. The crosses at the end of the curves indicate the total TBR probabilities, and the positions in n mark the TLE cutoffs corresponding to the appropriate densities.

threshold O in a transient plasma. Therefore, the TBR rates are expected to be strongly affected by the high n cutoff, and by the energy shift as well. The TBR rates are given for example by $\alpha_n^{TBR} \simeq 3.63\times 10^{-32} N n^4 g_n (1-e^{-x_n})/T_e\,(\mathrm{cm}^6/\mathrm{sec})$, where N is the electron density given in units of cm^{-3}, $x_n = 1/(2n^2 T_e)$, and T_e is in a.u. The degeneracy factor g_n is routinely taken to be $g_n \simeq n^2$, corresponding to the angular momentum degeneracy of states n. (Further discussion below.) The TBR probability is defined by

$$P^{TBR}(\mathrm{sec}^{-1}) \simeq N_e^2 \alpha_R^{TBR}\ (\mathrm{cm}^6/\mathrm{sec}). \tag{6}$$

Note the strong N^2 dependence of the TBR probability, as α_n^{TBR} is independent of N. Equations (5) and (6) may be compared for their N dependence. For some small N_e, RR can be faster than TBR.

The TBR probabilities obtained with $g_n \simeq n^2$ and the TLE cutoff are shown in Fig. 6(a). Four densities are considered, $N_e \simeq 10^5$, 10^7, 10^9, and $10^{11}\,\mathrm{cm}^{-3}$. In the case of $N_e \simeq 10^9\,\mathrm{cm}^{-3}$, the P's obtained with two alternate cutoffs $n'_{TL} = n_{TL}/\sqrt{2}$ and $n''_{TL} = \sqrt{2} n_{TL}$ are given, indicating typical range of uncertainty in the probability. Marked by double vertical bars in Fig. 6(a) are the minimum temperature as dictated by the TLE and Eq. (4). The values of P for $T_e < T_{e,\min}$ are useful when the equipartition involves neutrals as well, while the values for $T_e > T_{e,\min}$ may be used when $E_0 \geqslant 0$. For a confined plasma, Eq. (3) may have additional terms of either signs, that can further raise or lower the total E. Figure 6(b) shows the TBR probabilities as functions of n. The crosses at the top of the curves give the total P, obtained by summing over n. The sharp increase of P with n is of course due to the n^6 dependence of α_n^{TBR}.

The degeneracy factor g_n needs clarifications. The form $g_n \simeq 1$ was used earlier [8] to remedy the excessive contribution of the HRS to TBR, where the earlier formulas often gave unphysically large rates, even with the improved cutoff n_P. Furthermore, the maximum angular momenta that contribute to electron-ion collisions are usually limited to $l_{\max} \simeq 10$ to 15. In the case of RR at low energies, $l_{\max}$ was found [8] to be approximately $l_{\max} \simeq n/3$ for $n < 200$, which gives $g_n \simeq n^2/9$. Therefore, $g_n \simeq 1$ is an adequate choice that gives the total rates to within a factor of 100. This is relatively a small uncertainty as compared to the excessively large rates predicted previously with $g_n \simeq n^2$. Figure 7 shows the comparison between the TBR probabilities obtained with $g_n = n^2$ plus the TLE cutoff n_{TL} and the values estimated [8] with $g_n \simeq 1$ and a much larger cutoff given by $\min\{n_P, n_T\}$, where n_T is the thermal cutoff. Apparently, the choice $g_n \simeq 1$ provides more or less the correct total P's, but of course the n dependence (not shown in the figure) is poorly represented.

IV. AN EXPANDING PLASMA AND ADIABATIC MOTIONAL RECOMBINATION

When a plasma confining field is not present, CP expands under its own pressure, as observed in the experiment of Ref. [6]. As shown in Sec. II above and in Ref. [9], the expansion velocity v_I of the ions is given by $v_I \simeq \sqrt{(E_0 + \Delta_P)/M}$, where

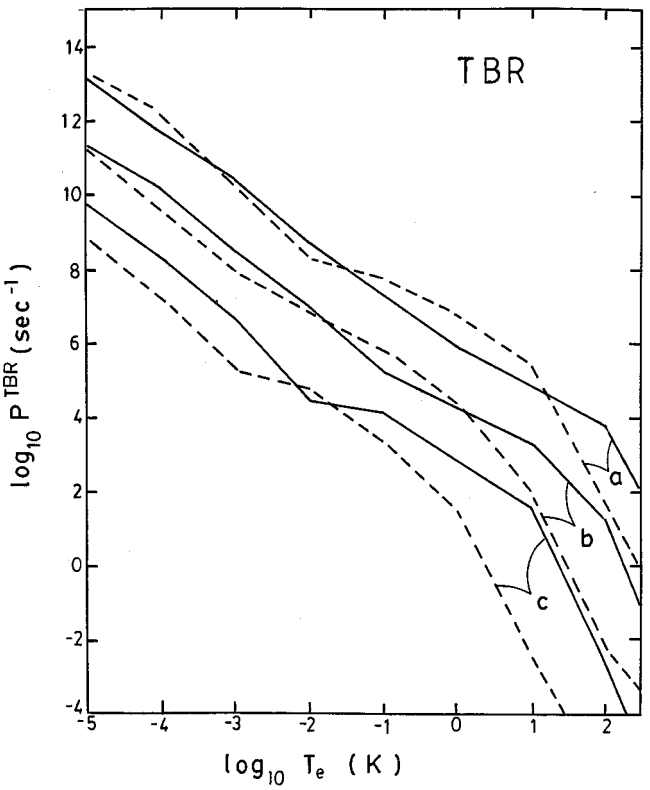

FIG. 7. Effects of two different choices for the degeneracy factor g_n on the total TBR probabilities are illustrated. The solid line is obtained with $g_n=n^2$ and the TLE while the dashed line is with $g_n\simeq 1$ and no TLE, as described in Ref. [9]. Note the quite good agreement between the two for low T. Of course, the n dependence of the probabilities is not correctly given by the choice $g_n\simeq 1$, especially for HRS. The TLE severely limits the role of HRS.

the TLE is represented by Δ_P in Eq. (3). Evidently, for $E_0 \ll \Delta_P$, the velocity depends only on Δ_P and thus on the ion density through the Wigner-Seitz radius a. Time scale of the expansion is given by the time required to have the interionic separation $2a$ increased by a factor of two, i.e., $\tau_a \simeq a\zeta/v_1$, where $\zeta=\mathbb{N}^{1/3}$ for the actual number $\mathbb{N}$ of ions in the plasma volume at $t=0$. For example, with the number of ions produced by laser ionization 10^6 and electron density of $10^7\ \mathrm{cm}^{-3}$, we have $\zeta\simeq 100$ and thus $\tau_a\simeq 10^{-5}$ sec. Since the thermalization time via *e-e* and *e-I* collisions is estimated to be [14,15] approximately 10^{-7} to 10^{-6} sec, respectively, we may assume that the thermalization has been completed before the plasma starts to expand. Incidentally, CP produced in laboratory may contain a sizeable population of neutrals, depending on the ionization efficiency. Although the *e-A* collision may be slow, we expect that some portion of the neutrals can acquire energies during the thermalization.

The TLE model of Sec. II provides a simple way to estimate the rates of electron capture due to the change in potential U. For this purpose, we define a time-dependent potential $-U_t(r)$ as

$$-U_t(r)\simeq -[1/r+1/(2a_t-r)]C_p, \tag{7}$$

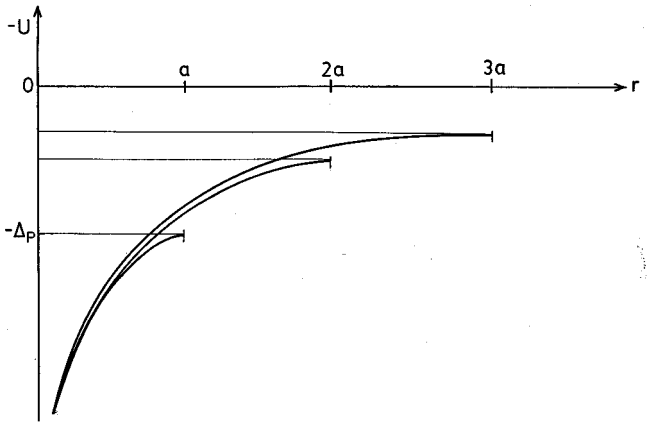

FIG. 8. The change in the potential $-U_t(r)$ as the plasma expands is illustrated. The time scale involved in the expansion is $\tau_a\simeq\zeta a/v_I$. Gradually, TLE and Δ are reduced with t, trapping the electrons that lie below the barrier around $r=a_t$.

with $a_t=a+v_It/\zeta$. This gives $\Delta_t\equiv U_t(r=a)=2C_P/a_t$. The variation of $-U_t$ with t is illustrated in Fig. 8, where the HRS levels are gradually recovered as the range and height of the barrier at $r=a_t$ increase.

Thermally distributed ions and electrons assume energies with respect to the shifted energy that starts from $-\Delta_P$, at the point O' in Fig. 1. We denote the electron energy by $\mathcal{E}_e=\Delta_P-\Delta_t$. Aside from the possible plasma edge effect, all the electrons with energy $\mathcal{E}_e\leqslant\Delta_P$ are below the original ionization threshold O. (By the plasma edge effect, we mean the field of the ions that are located at the edge of the plasma volume, which has no TLE as we move toward the outer region and thus retains the original threshold O.) As the plasma expands, the shift Δ_t will decrease with time, and eventually the original threshold is recovered at $a_t\to\infty$. Assuming a Maxwell distribution for the electrons, the probability of the electrons with energy $\mathcal{E}_e$ is $P(\mathcal{E}_e)d\mathcal{E}_e = 2\pi(\pi T_e)^{-1.5}e^{\mathcal{E}_e/T_e}\sqrt{\mathcal{E}_e}d\mathcal{E}_e$. On the other hand, from the definition of $\mathcal{E}_e(t)$, we have $d\mathcal{E}_e=(2C_Pv_I/a^2\zeta)dt$. A simple model for capture of trapped electrons as the plasma expands, is the adiabatic motional recombination (AMR)

$$P^{AMR}(t)=2\pi(\pi T_e)^{-1.5}e^{-\mathcal{E}_e/T_e}\sqrt{\mathcal{E}_e}2C_Pv_I/(a_t^2\zeta). \tag{8}$$

The probability P^{AMR} is plotted in Fig. 9 vs a_t for different N_e. The value $\zeta\simeq 47$ corresponding to $\mathbb{N}\simeq 10^5$ is used. Two different cases with $a=10^5$ and 10^6 a_B are treated. Also included are the estimates of the TBR probabilities for the two different densities. The lower curve is shown with a factor 100 multiplied to the actual values for plotting purpose.

The expression for P^{AMR} given by Eq. (8) is a crude first approximation. It may be improved for instance by a time-dependent perturbation theory in the adiabatic approximation. That is, with a perturbation $dU_t(r)/dt$, one has $\tilde{P}^{AMR}\simeq\int d\vec{r}\int dt\langle f|dU|dt|i\rangle e^{i\omega_{fi}t}$, where the initial and final states are defined in terms of the trapped electron orbitals in potential $-U$. Both adiabatic and impulse approximations may be examined. A recent paper [16] supports the trend predicted by Fig. 9, in which the role of TBR is minimal and the AMR

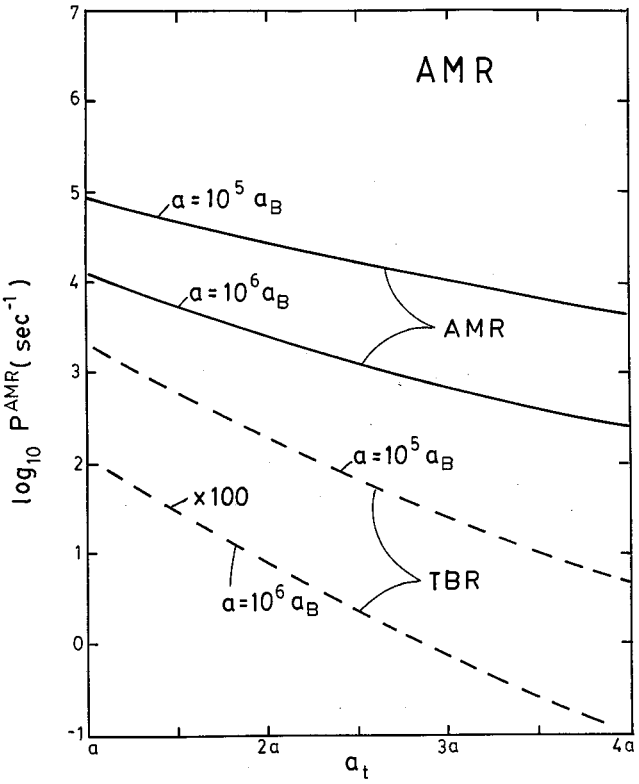

FIG. 9. The AMR probabilities P^{AMR} are given as functions of a_t for two different densities $N_e \simeq 10^9$ and $10^6\ \mathrm{cm}^{-3}$, corresponding to $a=10^5$ and $10^6\ a_B$. Also included are the TBR probabilities. The lower curve is for the lower density case, and is given with an extra factor of 100 for plotting purpose.

dominates as the plasma expands, including the quite distinct *n* distributions of the recombined states. It is also of interest to compare the AMR probability with that of RR given in Fig. 5.

V. DISCUSSION

Relaxation of an expanding CP is seen to proceed mainly by AMR, while the TBR should still be the dominant recombination mechanism for a confined plasma. After much adjustments in previous works [8], the TBR rates seem to have settled to values that may be reliable to within a factor of 10 at large Γ. Because of the strong cutoff of HRS contribution by the TLE, much of the complications in the TBR theory are avoided. However, improving the rates further would still require careful treatment of the electrons in both low energy continua and HRS. A better determination of g_n is also desirable, but is made less critical by the smaller cutoff n_{TL} than n_T and/or n_P. Recent experiments [16] seem to suport the general characteristics of AMR and TBR as predicted by Fig. 9, both in reduced magnitude of the TBR rates and the dominant role assumed by the AMR. The *n* dependence of the recombined ions also seem *s* to favor AMR.

The essential features of the TLE are expected to persist at higher *T* and larger *N*. But, the effect may be less conspicuous, as the energies involved are then much higher and Γ is much smaller (<0.01). For example, with $N_e \simeq N_I \simeq 10^{15}\,\mathrm{cm}^{-3}$, $a \simeq 10^3\, a_B$, and thus $\Delta_P \simeq 0.22$ a.u. $\simeq 0.4$ eV which may be compared with temperature of many eV.

From the discussion given in Sec. II, we have concluded that the CP without confining fields cannot achieve Wigner crystallization, because the necessary requirement of $\Gamma \simeq 150$ cannot be realized, as the TLE gives an upper bound, such that $\Gamma < 0.3$. We mention three possible ways to overcome this limitation:

(a) Manipulation of a confining field may give a higher density, without, at the same time raising the electron temperature.

(b) Plasma may be created with a ''negative'' E_0'. Instead of photoionizing directly to the continua, the trapped atoms may be excited to HRS levels with $n < \sqrt{\Delta_P}$ for given *a*. The excited atoms then interact with each other and emit Auger-type electrons and ionize, via Penning-like ionization [7]. The energy of the ejected electrons $\mathcal{E}_e$ then lies above the shifted threshold $-\Delta_P$ but stays below the original threshold at *O*, i.e., $\mathcal{E}_e \simeq \Delta_P$. Such a system may thermalize via electron-electron and electron-ion collisions, with much smaller $E = E_0' + \Delta_P < \Delta_P$, preferably at low density and the tails of the wave functions overlap.

(c) The neutrals in the plasma may effectively reduce the available *E* of Eq. (3) if the *e-A* collision can be enhanced, for example, by choosing atoms of very large polarizability. A buffer gas of such property may also help to lower *E*.

Evidently, the model constructed here, to estimate the TLE represented by Δ_P and the consequent AMR process for an expanding plasma, is crude and requires much refinements. A careful treatment of this exotic system by the density functional theory is desired.

[1] J. Weiner, V. S. Bagnato, S. Zilio, and P. S. Julienne, Rev. Mod. Phys. **71**, 1 (1999).
[2] F. Dalforo, S. Giorgini, S. Stringari, and L. P. Pitaevskii, Rev. Mod. Phys. **71**, 463 (1999).
[3] *Bose Einstein Condensation*, edited by A. D. Griffin, W. Snoke, and S. Stringari (Cambridge University Press, Cambridge, MA, 1995).
[4] T. C. Killian *et al.*, Phys. Rev. Lett. **83**, 4776 (1999).
[5] C. Orzel *et al.*, Phys. Rev. A **59**, 1926 (1999).
[6] S. Kulin *et al.*, Phys. Rev. Lett. **85**, 318 (2000).
[7] Y. Hahn, J. Phys. B **33**, L655 (2000).
[8] E. Zerrad and Y. Hahn, J. Quant. Spectrosc. Radiat. Transf. **59**, 637 (1998); Y. Hahn, Phys. Lett. A **231**, 82 (1997); **264**, 465 (2000).
[9] Y. Hahn, Phys. Lett. A (to be published).
[10] J. C. Stewart and K. D. Pyatt, Astrophys. J. **144**, 1203 (1966).
[11] M. W. C. Dharma-wardana and F. Perrot, Phys. Rev. A **26**, 2096 (1982).
[12] H. Xu and J. P. Hansen, Phys. Rev. E **57**, 211 (1998).
[13] S. Ichimaru, *Strongly Coupled Plasmas* (North-Holland, Am-

sterdam, 1990); *Strongly Coupled Plasma Physics*, edited by H. M. V. Horn and S. Ichimaru (University of Rochester Press, Rochester, NY, 1993).
[14] D. R. Nicholson, *Intro. Plasma Theory* (Krieger, NY, 1992).
[15] N. A. Krall and A. W. Trivelpiece, *Principles of Plasma Physics* (San Francisco Press, California, 1986).
[16] T. C. Killian, M. J. Lim, S. Kulin, R. Dumke, S. D. Bergeson, and S. L. Rolston, Phys. Rev. Lett. **86**, 3759 (2001).